Published in final edited form as:
Electrophoresis. 2011 September ; 32(17): 2358–2365. doi:10.1002/elps.201100020.

Dielectrophoretic Capture of *E. coli* Cells at Nanoelectrode Arrays

Lateef U Syed, **Jianwei Liu**, **Alex Price**, **Yi-fen Li**, **Christopher Culbertson**, and **Jun Li***
Department of Chemistry, Kansas State University, Manhattan, KS 66506

Abstract

This paper reports capture and detection of pathogenic bacteria based on AC dielectrophoresis (DEP) and electrochemical impedance spectroscopy (EIS) employing an embedded vertically aligned carbon nanofiber (VACNF) nanoelectrode array (NEA) vs. a macroscopic indium tin oxide (ITO) transparent electrode in “points-and-lid” configuration. The nano-DEP device was fabricated using photolithography processes to define an exposed active region on a randomly distributed NEA and a microfluidic channel on ITO to guide the flow of labeled *E. coli* cells, respectively, and then bond them into a fluidic chip. A high frequency (100 kHz) AC field was applied to generate positive DEP at the tips of exposed CNFs. Enhanced electric field gradient was achieved due to reduction in electrode size down to nanometer scale which helped to overcome the large hydrodynamic drag force experienced by *E. coli* cells at high flow velocities (up to 1.6 mm/sec). This DEP device was able to effectively capture a significant number of *E. coli*. Significant decrease in the absolute impedance (|Z|) at the NEA was observed by EIS experiments. The results obtained in this study suggest the possibility of integration of a fully functional electronic device for rapid, reversible and label-free capture and detection of pathogenic bacteria.

Keywords

Bacterial Capture; Dielectrophoresis; Dielectrophoretic Impedance Measurement; Nanoelectrode Array; Vertically Aligned Carbon Nanofibers

1 Introduction

Rapid detection of pathogens like bacteria and viruses is of great importance for monitoring water and food quality, the early detection and diagnosis of diseases, countering bioterrorism attacks, and other applications. Successful detection requires the manipulation and capture of pathogenic particles for further analysis. Optical tweezer [1,2], magnetic field [3,4], acoustic force [5], and surface interactions [6] have been used for this purpose. Another attractive approach is the use of electrical force such as electrophoresis (EP) and dielectrophoresis (DEP) [7–13]. DEP is of particular interest for capturing pathogenic particles stably in isolated locations of a device. The fundamental principles of DEP were described by Pohl in 1970s in dealing with the motion of a dielectric particle due to polarization effects in a nonuniform electric field [14]. DEP discriminates particles based upon their intrinsic dielectric properties which, to some extent, add selectivity in the manipulation of bioparticles from a heterogeneous mixture [15]. It has been extensively used as a nondestructive and noninvasive technique to detect and separate bacteria [16,17], discriminate between live and dead cells [8,18–20], detect isogenic mutants of *E. coli*

Correspondence: Dr. Jun Li, Department of Chemistry, Kansas State University, USA. junli@ksu.edu, Fax: 785-532-6666.

differing exclusively in one mutant allele [21], and capture and lyse smaller particles like viruses [22].

The time-average DEP force (F_{DEP}) on a spherical particle is given by [14]:

$$\langle F_{DEP} \rangle = 2\pi r^3 \varepsilon_m \mathrm{Re}[K(\omega)] \nabla E^2 \quad (1)$$

where r is the radius of the particle, ε_m is the permittivity of the suspending medium, ∇E^2 is the gradient of the square of the applied electric field strength, and Re[$K(\omega)$] is the real component of the complex Clausius-Mossotti (CM) factor given by:

$$K(\omega) = \frac{\varepsilon_p^* - \varepsilon_m^*}{\varepsilon_p^* + 2\varepsilon_m^*}; \quad \text{Where} \quad \varepsilon^* = \varepsilon - j\frac{\sigma}{\omega} \quad (2)$$

with ε^* representing the complex permittivity and the indices p and m referring to particle and medium respectively. σ is the complex conductivity, ω is the angular frequency ($\omega = 2\pi f$) of the applied electric field, and $j = \sqrt{-1}$. The value of Re[$K(\omega)$] lies between −0.5 and 1.0. If Re[$K(\omega)$]>0, particle experiences a positive F_{DEP} (pDEP) whereas if Re[$K(\omega)$]<0 the particle experiences negative F_{DEP} (nDEP).

Conventional DEP devices use patterned interdigitated electrodes (IDE) in which bacterial cells are mainly collected at the electrode edges [23,24]. However, in many applications one needs to manipulate single cells and preferably capture those cells at isolated spots instead of in aggregated form. Another problem associated with the IDE is that the electrodes are laid at the bottom of the fluidic channel and the ∇E^2 decreases rapidly further away from the channel bottom [25]. To deal with these problems, reversible DEP capture and release of a single *E. coli* employing NEA in “points-and-lid” geometry was developed [11]. Fabrication of well-controlled NEAs using VACNFs embedded in insulating materials on Si substrates has been reported earlier [26–28]. The exposed tips of VACNFs at the bottom Si substrate serve as a points array electrode and a large transparent indium-tin-oxide (ITO) electrode at the top acts as the lid. Recently it has been reported that precise e-beam lithographically patterned VACNFs can be fabricated as embedded NEAs on individually addressed micropads on the 4″ wafer scale [26–29]. This enables the use of embedded VACNF NEAs for either single or multiplex detection.

A critical factor for efficient cell trapping is the strength of F_{DEP} required to overcome the hydrodynamic drag force (F_{DRAG}) exerted on the cells by the fluidic flow which carries the cells moving downstream with fluid. F_{DRAG} could be considerably large at high flow velocities above 100 μm/s. The rationale behind the design of the DEP device in the present study is based on the results of DEP modeling performed using two-dimensional (2D) finite element multiphysics software [11]. According to this study, higher trapping efficiencies are attained either by injecting the particles at the height less than 3 μm from the NEA or by applying a high voltage bias above 9 V_{pp}. Efficient capture was observed at a high flow velocity up to 2 mm/sec. In the same study, a comparison of ∇E^2 and magnitudes of F_{DRAG} and F_{DEP} for particles located at different heights in the channel was made. In the middle of the fluidic channel, the direction of F_{DEP} (namely the vector of ∇E^2) is mostly in vertical direction, which is perpendicular to F_{DRAG} by the fluidic flow [11]. As a result, even a small DEP force is sufficient to deflect the bacterial particles downward as they flow by. But as the particle is moved closer to the NEA, a larger horizontal component in ∇E^2 starts to play a significant role which may exceed the horizontal drag force by the fluidic flow and retain the particles at the nanoelectrode site. It needs to be noted that, the opposite vertical drag force as the particles are pulled down by the initial vertical DEP force F_{DRAG} is neglected since the vertical velocity is negligible comparing to the high lateral flow velocity of the

fluid. It was found that, at a height of 2 μm, F_{DEP} is 3 orders of magnitude higher than the F_{DRAG} even at a high flow velocity of 10 mm/sec. If a particle is injected at the center of the channel, high trapping efficiencies even at very high flow velocities can be achieved.

This paper reports the fabrication of microfluidic device utilizing exposed tips of embedded VACNFs as nanoelectrodes in a selected area of 200 μm × 200 μm to capture bacterial cells of *E. coli* strain DHα5. The active area is defined by a 2-μm thick SU-8 photoresist to minimize the step effects as *E. coli* cells flow in the channel into the exposed NEA area. This avoided the complication in the previous study [11] that *E. coli* cells may be preconcentrated by DEP at the VACNF NEA surface before entering the microscope's field of view. It has been reported that the electric field (e-field) can be enhanced with the high-aspect-ratio non-planar structure as offered by fiber-like nanoelectrodes (NEs) both in vacuum [30–32] and in solution [11,33]. We demonstrate here that the attractive nanoscale "point-and-lid" design and the great enhancement in e-field gradient lead to effective capture of *E. coli* at a high flow velocity up to 1.6 mm/sec. The DEP capture of *E. coli* cells at different AC frequencies and flow velocities are investigated which provides optimized DEP conditions apparently different from the previous study [11]. Towards our goal of label-free electrical detection using dielectophoretic impedance measurements (DEPIM), we performed the initial electrochemical impedance spectroscopy (EIS) studies. Significant decrease in the value of |Z| was observed at the optimum DEP frequency of 100 kHz, upon capture of *E. coli* cells at the CNF NE tips. Thus it is highly feasible for real-time monitoring the capture process by DEPIM.

2 Experimental Methods

2.1 DEP Device Fabrication

Fabrication of the nano-DEP device (see Supporting Information Fig. S1a) involves five major steps. The details of each step are as follows:

1. Embedded VACNF NEAs were made by the method described before [26,34]. Briefly, ~100 nm of chromium and ~22.5 nm nickel catalyst were deposited on a 1 cm × 2 cm silicon (100) wafer covered with 500 nm of thermal oxide (Si-Tech, Inc, Topsfield, MA) using ion sputtering (Gatan 681). Plasma enhanced chemical vapor deposition (PECVD) (Aixtron) was used to grow brush-like VACNFs. A ~15 min growth yields VACNFs with ~100 nm in diameter and ~5 μm in length. Dielectric SiO_2 was then deposited on as-grown VACNFs by thermal chemical vapor deposition (CVD) using tetraethylorthosilicate (TEOS) as a precursor. SiO_2 encapsulates the bottom Cr layer and each individual CNF. It also adds mechanical strength to the CNFs. The embedded CNF chip is then polished manually using 0.3 μm Alpha micropolish alumina (Buehler, Lake Bluff, IL) for 2 hrs to planarize the surface. Reactive ion etching (RIE) (Nano-Master, NRE3000) with CHF_3 etchant was then used to etch away SiO_2 from top and expose the tips of CNFs. After RIE, NEA chip was soaked in 1.0 M HNO_3 for 10 min to dissolve Ni catalyst from the exposed tips and then polished manually with 0.05 μm micropolish alumina for ~2 min to clean up the debris formed during RIE.
2. SU-8 2002 photoresist (Microchem, Newton, MA) of ~2.0 μm in thickness was used to develop patterns on the planarized NEA (see Fig. 1a). The substrate was cleaned by rinsing with acetone several times, blow-dried in air and dehydrated at 150 °C for 20 min in an oven (Fisher Scientific, 3510-1FS). SU-8 2002 was spin coated on NEA chip at 2800 rpm speed for 40 sec using a spin coater. It was soft-baked at 95 °C for 75 sec on a hot plate, exposed to UV light (44 mW/cm^2) for 3 sec through a Mylar mask in soft contact mode to define a 200 μm × 200 μm active area, post baked for 90 sec on a hot plate at 95 °C, developed in SU-8 developer,

and washed with isopropyl alcohol (IPA) and dried using a stream of dry N_2. This provides the capability to study DEP effects only in the small selected area in contrast to the previous study [11] which was complicated by the fact that NEAs were exposed at the bottom of the whole fluidic channel. It is also an important step toward future studies requiring individually addressed multiplex DEP arrays.

3. SU-8 2010 photoresist (Microchem, Newton, MA) of ~18 μm in thickness (see Fig. 1a) was deposited on a 2 cm × 4 cm ITO-coated glass electrode (Delta Technologies, MN) by spin coating SU-8 2010 at 1350 rpm speed for 40 sec. It was then soft baked at 95 °C for 4 min on a hot plate, exposed to UV light (44 mW/cm^2) for 5.7 sec through the second Mylar mask to define the microchannel (500 μm × 18 μm (WxH)) and the circular chamber (~2 mm in diameter and 18 μm in height), post baked for 4 min at 95 °C on a hot plate. The remaining steps were the same as explained for NEAs. Finally, two holes were drilled from glass side using a 0.75 mm diameter diamond drill bit at the two ends of the microchannel and then a section (1 cm × 2 cm) of ITO-glass electrode containing the microchannel was diced to eliminate edge-beads, which may interfere with the bonding process.

4. SU-8 patterned NEA and ITO-glass electrodes were cleaned with IPA to remove dust particles. They were aligned under a stereo microscope with a 4× objective lens and then pressed with a mechanical force (see Fig. 1a and 1b). The substrates were then placed in a vacuum oven (Curtin Matheson Scientific, Inc) which was preheated to 175 °C. It was evacuated and held at 25 Torr for ~20 min for the substrates to bond with each other.

5. Electrical connections to the electrical pads on the NEA and ITO-glass were made using conductive silver epoxy (MG Chemicals, Ontario) and thirty gauge wires. Microbore tubing was used to connect a 1 ml glass syringe to the DEP device using sleeves, ferrules and fittings (Upchurch Scientific Inc, WA). A syringe pump (NE-1000, New Era Pump Systems, Inc) was used to control the flow rate during the experiments.

2.2 *E. coli* Cell Culture and Labeling

Frozen *E. coli* DHα5 stock was purchased from Fisher (18265-017) and grown in LB medium in a sterile culture tube and incubated overnight at 37 °C to reach a cell concentration of ~1×10^9 cells/ml into the late log phase. The cells were centrifuged at 5000 rpm for 5 min and supernatant LB media was discarded. The collected cells were resuspended and washed in ~1.5 ml 1X phosphate buffer saline (PBS) at least 3 times to eliminate the remaining ingredients of the LB media. Labeling of *E. coli* cells was done in two steps. In first step, ~3×10^9 cells/ml were incubated with FITC conjugated rabbit anti-*E. coli* Ab (AbD Serotech, NC) at 330 μg/ml for 1 hr at room temperature (RT). The cells were then centrifuged, and washed 3 times with PBS. In the second step, *E. coli* cells were incubated with Alexa 555 conjugated goat anti-rabbit second Ab (Invitrogen, CA) at 130 μg/ml for 1 hr at RT. The labeled *E. coli* cells were pelleted and washed 2 times with 1X PBS followed by 2 times with deionized (DI) water. The cells were finally resuspended in DI water to a desired concentration of ~1×10^9 cells/ml for DEP experiments.

2.3 DEP Experiments

An upright fluorescence optical microscope (Axioskop 2 FS plus; Carl Zeiss) in reflection mode was used for DEP experiments. The packed fluidic chip was placed under the 50× objective and focused at 200 μm × 200 μm active NE area through the transparent ITO-glass electrode (see Supporting Information Fig S1b). A filter set with excitation wavelength of 540–552 nm and emission wavelength of 567–647 nm (filter set 20HE, Carl Zeiss) was

used in connection with an Axio Cam MRm digital camera to record fluorescence videos at an exposure time of 0.4 s using multi-dimensional acquisition mode in the Axio-vision 4.7.1 release software (Carl Zeiss MicroImaging, Inc). Before performing DEP experiments 1.0 ml BSA solution (2% w/v) was fed through the channel at a flow rate (Q) of 0.2 μl/min to passivate the surface of SU-8 and SiO_2 in the fluidic channel in order to prevent non-specific adsorption of *E. coli* cells. This was found critical in avoiding biofouling so that the DEP device can be reliably used over months. The channel was then washed with 2 ml DI water at a $Q = 5.0$ μl/min. Labeled *E. coli* suspension in DI water was injected into the channel. DEP experiments at different frequencies (f) of the sinusoidal AC voltage and at different flow velocities of *E. coli* cells were performed. Each experiment was performed for a span of 30 sec during which no voltage (V_{off}) was applied in the initial ~10 sec, fixed AC voltage at different frequencies was applied (V_{on}) in the next ~10 sec, and no voltage was applied (V_{off}) in the last ~10 sec. Videos were recorded during each experiment. The response of *E. coli* cells was also visually monitored using microscope to determine the optimum frequency of the AC voltage for DEP capture of *E. coli* cells. DEP videos were later analyzed using Automeasure module in Axio vision software (Carl Zeiss) to quantify the number of isolated and fixed bright spots each of which corresponds to a single captured *E. coli* cell. This provides direct cell counting in contrast to the arbitrary quantification in the previous study [11] using integrated fluorescence intensity over the video frames. In addition, the true linear flow velocities within the focal depth of the microscope from NEA surface in the 200 μm × 200 μm active area was calculated from the recorded videos (see Supporting Information videos for details), which avoided the large errors by using average flow velocities in the previous study [11].

2.4 Electrochemical Impedance Spectroscopy Experiments

EIS was measured in a two-electrode setup before and after *E. coli* cells were captured by DEP using a potentiostat (PARSTAT 2273, Princeton Applied Research Corporation) with *E. coli* cells suspended in DI water and filled between the CNF NEA and the ITO-glass electrode in the microfluidic channel. An AC voltage of 2.8 V_{pp} (peak-to-peak voltage, the upper limit of the instrument) was applied at the CNF NEA at the open-circuit potential (~1–100 mV) vs. the ITO-glass electrode with the frequency uniformly spanned in the logarithm scale from 1 MHz to 100 mHz. The applied voltage amplitude is much larger than the value of 10–50 mV_{pp} used in conventional EIS measurements since our goal is at developing real-time impedance measurements in which the AC voltage serves both as the DEP driving force and the EIS probe. For capturing, *E. coli* cells were injected into the fluidic channel at a flow velocity of 0.11 mm/sec. The pDEP was applied for 5–10 seconds with an AC voltage of 10 V_{pp} using a wave function generator (Model 33120A, Hewlett Packard) at a fixed frequency of 100 kHz. After capturing enough *E. coli* cells, the flow was turned off while the AC voltage remained on for ~10 minutes. Sufficient number of *E. coli* cells were observed by fluorescence microscope to stick to the exposed tips of the CNF and remained stably attached after the AC voltage was turned off. The cell was then disconnected with the solution sealed in the channel by two inline valves and moved to the potentiostat for EIS measurements.

3 Results and Discussion

To achieve efficient bacterial capture at a selected location, a square area of 200 μm × 200 μm was opened in a 2-μm thick SU-8 2002 coating on the NEA substrate in this study. A microchannel of ~18 μm in height was patterned in the 18 μm thick SU-8 2010 layer on ITO-glass electrode. The height of the feature in the SU-8 films on the NEA and the ITO-glass were measured using Ambios Technology XP-2 profiler and was consistent with the design (see Supporting Information Fig. S2). A bright field image of the DEP device with the active NEA square at the bottom and a microchannel with the circular chamber in the

SU-8 on the ITO-coated glass on top is shown in Fig. 1a (also see Supporting Information Fig. S1a). The inset shows an enlarged cross-sectional schematic of the F_{DRAG} and F_{DEP} on a single *E. coli* cell as it flows through the channel above the active NEA square. A cross-sectional view of the structure of the DEP device is further schematically shown in Fig. 1b. Fluid enters from one end and collected in a waste collector at the other end. The top-view SEM image of the surface of a CNF NEA is shown in Fig. 1c. The average diameter of exposed CNFs is ~100 nm, the density is ~2×10^7 CNFs/cm^2, and the average spacing is ~2.0 μm. At such low density, the exposed CNF tips are well separated from each other and each is expected to behave same as a single NE. The DEP device has a shelf life of few months, can be used multiple times and its behavior was observed to be normal.

The captured *E. coli* cells at each exposed CNF tip appear as round bright spots as shown in the enlarged schematic of the device in Fig. 1a. As the AC voltage is turned-off the captured *E. coli* cells are released and dragged away by the hydrodynamic force F_{DRAG} from the fluidic flow. To stably capture the cells, the F_{DEP} has to somehow overcome F_{DRAG} acting on an *E. coli* cell. When an AC voltage of proper frequency is applied to the CNF NEA, *E. coli* cells will be pulled by the pDEP force toward the exposed tips of NEA and remain captured as long as the AC voltage is on. DEP capture experiments at various AC frequencies (50 kHz to 1 MHz) at fixed AC amplitude of 10 V_{pp} were first carried out. The number of captured *E. coli* cells is quantified by counting the number of fixed bright spots using Automeasure module (Carl Zeiss). Fig. 2 plots the number of bright spots at various AC frequencies. It can be observed that there is least number (~30) of bright spots at 1 MHz frequency whereas the count was maximum (~300) at 100 kHz, indicating more *E. coli* cells being captured at the NEA. Clearly, 100 kHz gives the best capture efficiency for pDEP capture of *E. coli* cells. The 1 MHz AC voltage used in the previous study [11] was apparently too high and far from the optimum condition.

We then carried out pDEP capture experiments with AC voltage at 10 V_{pp} and the frequency at 100 kHz while sequentially increasing the flow velocity of *E. coli* cells from 0.11 mm/sec to 1.6 mm/sec. The flow velocities referred is the linear flow velocities at the 200 μm × 200 μm NEA area calculated from the recorded videos (see Supporting Information videos for details). Before applying DEP, *E. coli* cells were flowed through the channel for sufficient time to get rid of air bubbles and other particles to attain a uniform and stable flow. Fig. 3a shows snap shot of the video as *E. coli* cells are flowing at 0.11 mm/sec through the channel when the AC voltage is off, where each cell appears as a stretched line. Pseudocolor is used to represent the fluorescence emission. Almost immediately after the voltage is turned on, the stretched lines turn into bright round spots at fixed positions as shown in Fig. 3b, indicating that *E. coli* cells are captured at the tips of CNF NEA by pDEP. When the flow velocity is increased, *E. coli* cells experience a larger F_{DRAG} since F_{DRAG} is proportional to the flow velocity. As a result, less *E. coli* cells can be stably captured. Fig. 3c shows a snap shot from a video of *E. coli* cells flowing at a flow velocity of 1.6 mm/sec when the voltage is turned-off. *E. coli* cells appear as much longer stretched lines due to the higher flow velocity as compared to that in Fig. 3a. When the voltage is turned on, substantial *E. coli* cells are captured by pDEP as seen in Fig. 3d. This indicates that the pDEP force is sufficient to attract many cells (mostly those close to the NEA surface) toward the NEA. Once they are at the CNF tip, the lateral DEP force component is larger than the hydrodynamic drag force along the flow direction even at a high flow velocity of 1.6 mm/sec and thus is able to keep the *E. coli* cell at the surface.

Further analysis was carried out to show the capture kinetics at three different flow velocities. The number of bright spots at each time frame was counted during DEP capture experiments and plotted vs. time in Fig. 4a. At the initial conditions at all three flow velocities, almost no *E. coli* cell is trapped when no AC voltage is applied, the moment an

AC voltage is applied, a sudden increase in the count of bright spots is seen, indicating the capture of *E. coli* cells at the NEA. The count remains almost the same during the time the voltage is applied but it clearly depends on the flow velocity. At a low flow velocity of 0.11 mm/sec, the count of bright spots is ~300 while it sharply drops to ~70 as the flow velocity is increased to 1.6 mm/sec. More details of the kinetic process to capture *E. coli* cells can be seen in real-time DEP videos at 0.11 mm/sec and 1.6 mm/sec flow velocities in Supporting Information. The flow velocity at 1.6 mm/sec is ~3 times higher than the maximum flow velocity of 0.5 mm/sec that is reported for a micro-points-and-lid device [35] and is at the high end of the typical range of the flow velocity (0.04–2 mm/sec) used in interdigitated micro-DEP device [36].

For stable capture of a particle, two sequential processes are involved. First, a vertical DEP force has to be strong to quickly pull the particle to the NEA tip before it flows out of the active area. Second, the lateral DEP force F_{DEP} at the NEA tip has to overcome the drag force F_{DRAG} by the lateral fluidic flow which is defined by Stokes equation [36]:

$$F_{drag}=6\pi kr\eta\upsilon_m, \quad (3)$$

where η is the dynamic viscosity of the fluid, υ_m is the velocity of the medium fluid at the center of the particle, and k (>1) is a nondimensional factor accounting for the wall effects. It should be noted that the value of υ_m is height-dependent since the fluid follows in a parabolic laminar flow profile with the highest velocity at the center and slowest velocity at the channel walls. In this study, the flow velocity is calculated from the cell movement in the videos recorded at the CNF NEA surface at the bottom of the microchannel, and thus it is the actual υ_m within the depth of field of the camera (~0.6 μm by the tutorial calculator at Carl Zeiss website) from the CNF NEA surface. The average flow velocity $<\upsilon_m>$ is ~2.78 mm/sec (see Supporting Information), much higher than 2.0 mm/s used in the previous study [11]. From Eq. (3), increasing the flow velocity clearly does not favor pDEP capture of the bacterial cells. However, many practical applications require rapidly isolating bacterial cells from a dilute solution, in which a high flow rate has to be used to obtain sufficient throughput. It has been very challenging to use pDEP for such applications. The pDEP force has to be increased to compete with the increased drag force. According to the previous DEP modeling study [11], the magnitude of ∇E^2 at the NE tip is 200 times higher than that of the micro electrodes used in points-and-lid configuration. This provides a very large DEP force required to counteract the drag force and capture *E. coli* stably at the CNF NEA. Here we show a systematic study at a series of surface flow velocities from 0.11 mm/sec to 1.6 mm/sec. It is convincing that pDEP capture of *E. coli* cells is still effective at the flow velocity of 1.6 mm/sec or even higher.

The kinetic profiles of the fluorescent spots vs. time during pDEP capture of E. coli cells in our study can be interestingly compared with those in the previous study [11]. Arumugam et al found that, at low AC voltage amplitude (1–7 V_{pp}), there was a slow kinetic process which took seconds for the fluorescence intensity from captured *E. coli* cells to reach the saturated level. But it almost immediately jumped to the saturated level at a high AC voltage of 9 V_{pp}. The fast kinetic phenomena at 9 V_{pp} is consistent with our results in Fig. 4a, which were all measured at 10 V_{pp} AC bias. Interestingly, although the saturated fluorescence counts varies with the flow velocity, none of the curves shows the slow kinetic process during which bacterial cells slowly accumulates when the AC voltage is turned on. It seems that pDEP action is accomplished instantaneously even at the highest flow velocity. The number of saturated fluorescent spots is plotted vs. the flow velocity in Fig. 4b. A monotonically decreasing curve is obtained as the flow velocity is increased. The trend is consistent with our discussion above. It would be interesting to derive some models to

simulate the experimental results in both kinetics and flow-velocity dependence in the future.

Our long-term goal is to develop this technique as a rapid pathogen detection technique using handheld electronics. The fluorescence measurement needs to be replaced with simpler electronic methods for detection. Impedance biosensors integrated with techniques like DEP, termed as DEPIM, are widely employed for rapid detection of pathogenic bacteria. DEPIM has been demonstrated to monitor the processes utilizing pDEP force to capture bioparticles on the electrode surface at a fixed AC frequency [37]. It can detect pathogenic bacteria both quantitatively and selectively at IDEs where the bacteria are trapped in between the electrode pair in a pearl chain fashion and cause the conductance change [20,38].

To explore the feasibility of DEPIM with CNF NEAs, we carried out EIS measurements with 2.8 V_{pp} AC voltage bias (the maximum afforded by the potentiostat) before and after pDEP capture of *E. coli* cells. The Bode plots of EIS over the whole frequency range are shown in Fig. 5a. The data after pDEP is performed at 10 V_{pp} (with a function generator) is compared with that without subjected to pDEP capture. The enlarged plot in Fig. 5b shows that the |Z| value of the CNF NEA in *E. coli* suspension at 100 kHz (the optimum pDEP frequency) is ~1627 Ω before pDEP bacterial capture. After running pDEP experiments to capture *E. coli* cells, the |Z| value decreases to ~684 Ω (by ~58%). The decrease in the impedance is likely because the large (1–2 μm in size) and more conductive bacterial cells are in direct contact with the small CNF tips (~100 nm in dia.), equivalent to increasing the electrode size. The results in this study serve as a reference of the maximum change that one can obtain to reach the saturated bacterial capture. In future studies, further EIS study will be carried out at varied capture quantities and real-time impedance change at a fixed AC frequency (i.e. DEPIM) will be explored at different cell concentrations and flow velocities.

4 Concluding remarks

In summary, we report effective pDEP capture of *E. coli* cells from a high-velocity flow at the exposed tips of an embedded CNF NEA. The CNF NEA is placed at the bottom of a microfluidic channel vs. a large transparent ITO-coated glass at the top with 20 μm spacing in between to form a “points-and-lid” configuration. Our results have confirmed the observations in a previous report using such nano-DEP device [11]. More importantly, we found that the optimum frequency of the AC voltage is around 100 kHz, much lower than 1 MHz used in the previous study. *E. coli* cells can be captured in a selected area by lithographically defining a window on the CNF NEA chip. The total quantity of captured *E. coli* cells is found to decrease monotonically as the flow velocity is increased. Interestingly, the fluorescence signal representing the captured *E. coli* cells immediately jumps to the saturated level at all flow velocities once a 10 V_{pp} AC bias is applied. No kinetic accumulation is observed at such a high-voltage bias. EIS before and after capturing *E. coli* cells show clear changes over the whole frequency range. Particularly, the |Z| value at 100 kHz (the optimum pDEP operation condition) is decreased by ~58% after cell capture. Therefore, it is highly feasible to use real-time impedance (i.e. DEPIM) for directly monitoring pDEP capture of bacterial cells.

Supplementary Material

Refer to Web version on PubMed Central for supplementary material.

Acknowledgments

JL thanks Kansas State University and Early Warning Inc. for financial support. Part of this work was supported by Grant Number P20RR015563 from the National Center for Research Resources. A support from Johnson Center for Basic Cancer Research at Kansas State University was also instrumental in acquiring the facilities used in this work. We thank Dr. Daniel Higgins for helpful discussions during the manuscript preparation.

Abbreviations

AC	Alternating Current
CM	Clausius-Mossotti
CNF	Carbon Nanofiber
DEP	Dielectrophoresis
DEPIM	Dielectrophoretic Impedance measurement
EIS	Electrochemical Impedance Spectroscopy
NE	Nano Electrode
NEA	Nano Electrode Array
VACNF	Vertically Aligned Carbon Nanofiber

References

1. Svoboda K, Block SM. Annu Rev Biophys Biomol Struct. 1994; 23:247–285. [PubMed: 7919782]
2. Enger J, Goksor M, Ramser K, Hagberg P, Hanstorp D. Lab Chip. 2004; 4:196–200. [PubMed: 15159778]
3. Berger M, Castelino J, Huang R, Shah M, Austin RH. Electrophoresis. 2001; 22:3883–3892. [PubMed: 11700717]
4. Yapici MK, Ozmetin AE, Zou J, Naugle DG. Sens Actuator A-Phys. 2008; 144:213–221.
5. Wu JR. J Acoust Soc Am. 1991; 89:2140–2143. [PubMed: 1860996]
6. Jung DR, Kapur R, Adams T, Giuliano KA, et al. Crit Rev Biotechnol. 2001; 21:111–154. [PubMed: 11451046]
7. Voldman J. Annu Rev Biomed Eng. 2006; 8:425–454. [PubMed: 16834563]
8. Lapizco-Encinas B, Simmons B, Cummings E, Fintschenko Y. Electrophoresis. 2004; 25:1695–1704. [PubMed: 15188259]
9. Klodzinska E, Buszewski B. Anal Chem. 2009; 81:8–15. [PubMed: 19125448]
10. Desai MJ, Armstrong DW. Microbiol Mol Biol Rev. 2003; 67:38–51. [PubMed: 12626682]
11. Arumugam PU, Chen H, Cassell AM, Li J. J Phys Chem A. 2007; 111:12772–12777. [PubMed: 17999481]
12. Durr M, Kentsch J, Muller T, Schnelle T, Stelzle M. Electrophoresis. 2003; 24:722–731. [PubMed: 12601744]
13. Arai F, Ichikawa A, Ogawa M, Fukuda T, et al. Electrophoresis. 2001; 22:283–288. [PubMed: 11288895]
14. Pohl, HA. The behavior of neutral matter in nonuniform electric fields. Cambridge Univ. Press; Great Britain: 1978. Dielectrophoresis.
15. Çetin B, Li D. Electrophoresis. 2010; 31:3035–3043. [PubMed: 20872609]
16. Betts WB. Trends Food Sci Technol. 1995; 6:51–58.
17. Hughes MP. Electrophoresis. 2002; 23:2569–2582. [PubMed: 12210160]
18. Suehiro J, Hamada R, Noutomi D, Shutou M, Hara M. J Electrostat. 2003; 57:157–168.
19. Lapizco-Encinas BH, Simmons BA, Cummings EB, Fintschenko Y. Anal Chem. 2004; 76:1571–1579. [PubMed: 15018553]

20. Suehiro J, Noutomi D, Shutou M, Hara M. J Electrostat. 2003; 58:229–246.
21. Castellarnau M, Errachid A, Madrid C, Juarez A, Samitier J. Biophys J. 2006; 91:3937–3945. [PubMed: 16950844]
22. Park K, Akin D, Bashir R. Biomed Microdevices. 2007; 9:877–883. [PubMed: 17610069]
23. Suehiro J, Ohtsubo A, Hatano T, Hara M. Sens Actuator B-Chem. 2006; 119:319–326.
24. Liju Y, Banada PP, Chatni MR, Kwan Seop L, et al. Lab Chip. 2006; 6:896–905. [PubMed: 16804594]
25. Crews N, Darabi J, Voglewede P, Guo F, Bayoumi A. Sens Actuator B-Chem. 2007; 125:672–679.
26. Li J, Koehne JE, Cassell AM, Chen H, et al. Electroanalysis. 2005; 17:15–27.
27. Tu Y, Lin YH, Yantasee W, Ren ZF. Electroanalysis. 2005; 17:79–84.
28. Baker SE, Tse KY, Lee CS, Hamers RJ. Diamond Relat Mater. 2006; 15:433–439.
29. Arumugam PU, Chen H, Siddiqui S, Weinrich JAP, et al. Biosens Bioelectron. 2009; 24:2818–2824. [PubMed: 19303281]
30. Edgcombe CJ, Valdre U. J Microsc-Oxford. 2001; 203:188–194.
31. Guillorn MA, Hale MD, Merkulov VI, Simpson ML, et al. Appl Phys Lett. 2002; 81:2860–2862.
32. Teo KBK, Minoux E, Hudanski L, Peauger F, et al. Nature. 2005; 437:968. [PubMed: 16222290]
33. Tuukkanen S, Toppari JJ, Kuzyk A, Hirviniemi L, et al. Nano Lett. 2006; 6:1339–1343. [PubMed: 16834407]
34. Li J, Ng HT, Cassell A, Fan W, et al. Nano Lett. 2003; 3:597–602.
35. Gray DS, Tan JL, Voldman J, Chen CS. Biosens Bioelectron. 2004; 19:1765–1774. [PubMed: 15198083]
36. Li H, Zheng Y, Akin D, Bashir R. Microelectromech Syst. 2005; 14:103–112.
37. Yang L, Bashir R. Biotechnol Adv. 2008; 26:135–150. [PubMed: 18155870]
38. Suehiro J, Yatsunami R, Hamada R, Hara M. J Phys D-Appl Phys. 1999; 32:2814–2820.

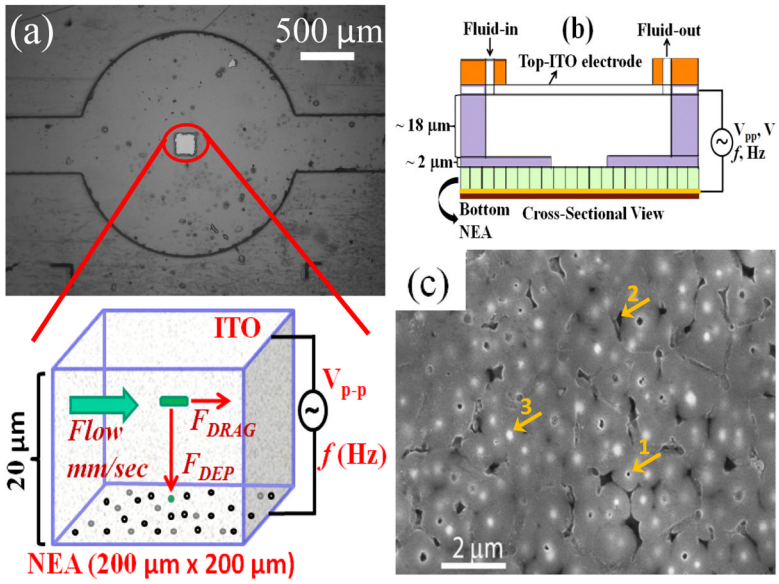

Figure 1.

Design of nano-DEP device. (a) A brightfield image of a nano-DEP device. The small square (200 µm × 200 µm) at the center is the exposed active CNF NEA placed at the bottom. The inset beneath shows the enlarged schematic of an *E. coli* cell influenced by the major forces when it flows through the channel between the two electrodes where a AC voltage is applied. The total height of the channel is 20 µm. (b) Cross-sectional schematic view of the nano-DEP-device. (c) A SEM image (top view) of the CNF NEA with arrow 1 indicating an exposed CNF tip, arrow 2 as a void in SiO_2 matrix, and arrow 3 for unexposed CNF tip.

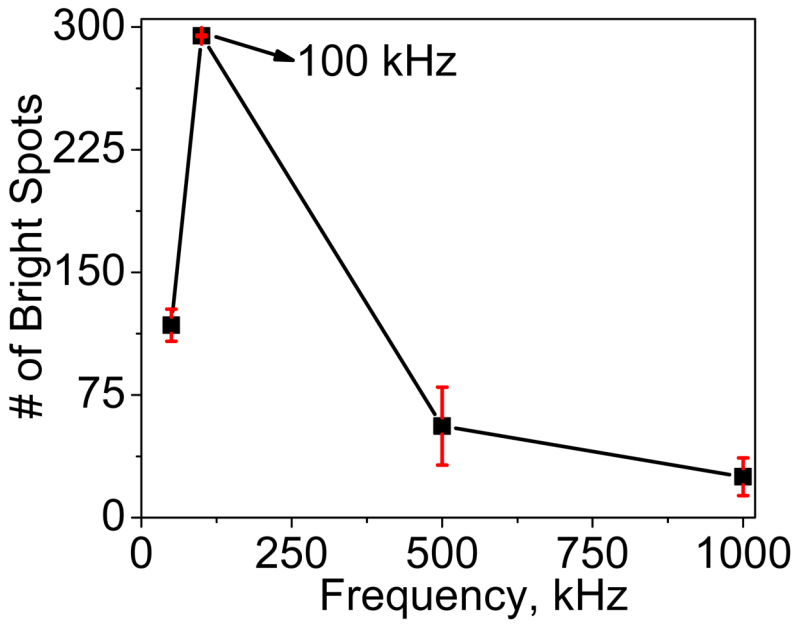

Figure 2.
The count of bright spots in pDEP experiment vs. the frequency of the applied AC voltage. All experiments use an AC voltage bias of 10 V_{pp}. The maximum trapping efficiency is obtained at 100 kHz.

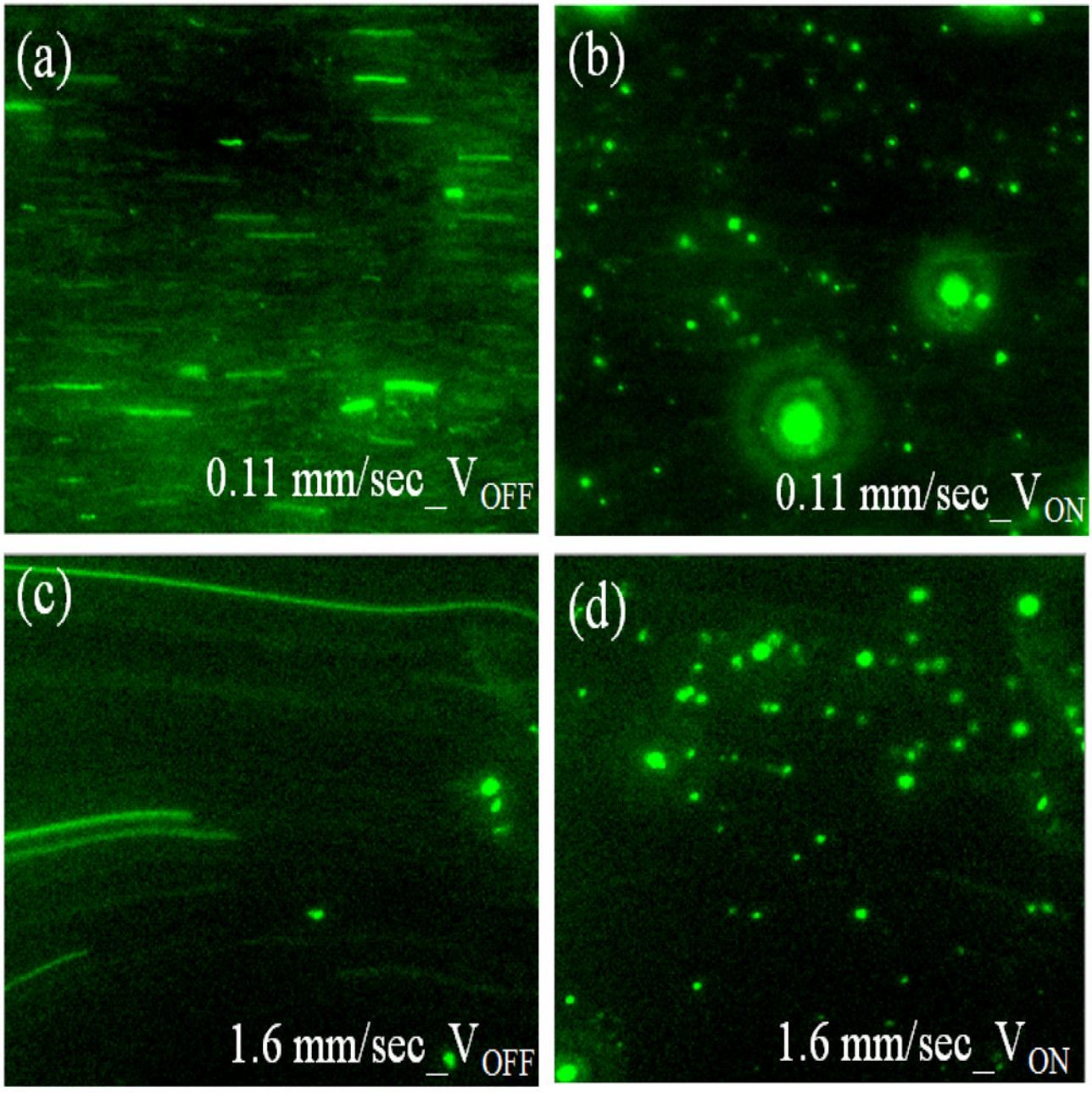

Figure 3.
Images of *E. coli* cells before and after being captured at the CNF NEA with 100 kHz frequency and 10 V_{pp} AC bias. (a) and (c) Snap shots of *E. coli* cells flowing at 0.11 and 1.6 mm/sec flow velocities, respectively, in the DEP device when no voltage is applied. (b) and (d) Snap shots of *E. coli* cells captured at the exposed tips of CNF NEA by applying an AC voltage of 10 V_{pp} at 0.11 and 1.6 mm/sec flow velocities, respectively.

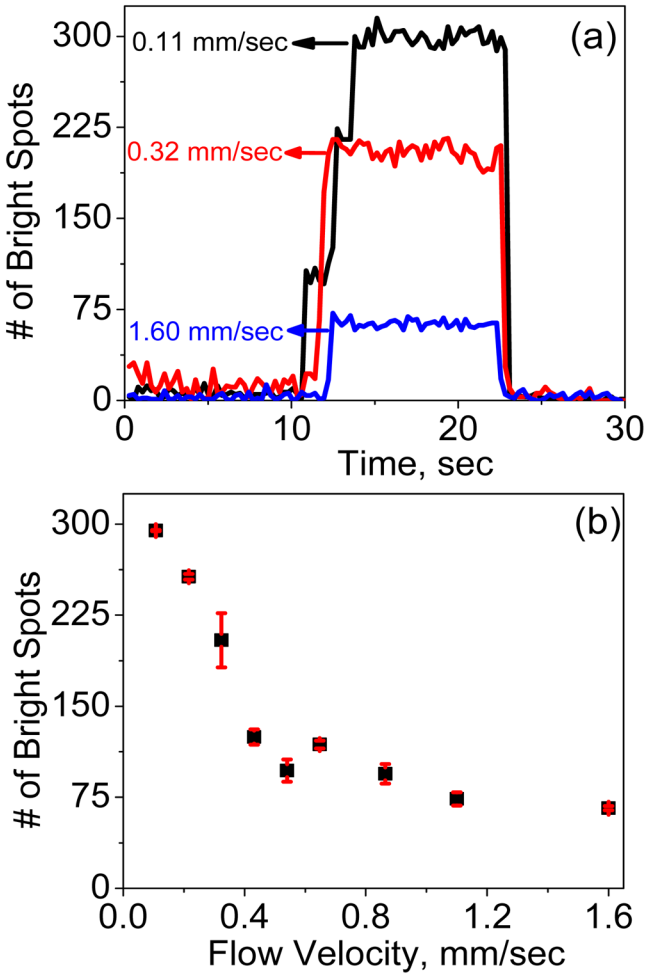

Figure 4.

Quantifying *E. coli* cells captured at different flow velocities. (a) The change in number of captured *E. coli* cells (correlated to the number of bright spots counted) with respect to time at three flow velocities (0.11, 0.32 and 1.6 mm/sec). DEP capture experiments are performed by applying an AC voltage of 10 V_{pp} at a frequency of 100 kHz. (b) The change in number of bright spots as a function of flow velocity as *E. coli* cells are flowing through the channel.

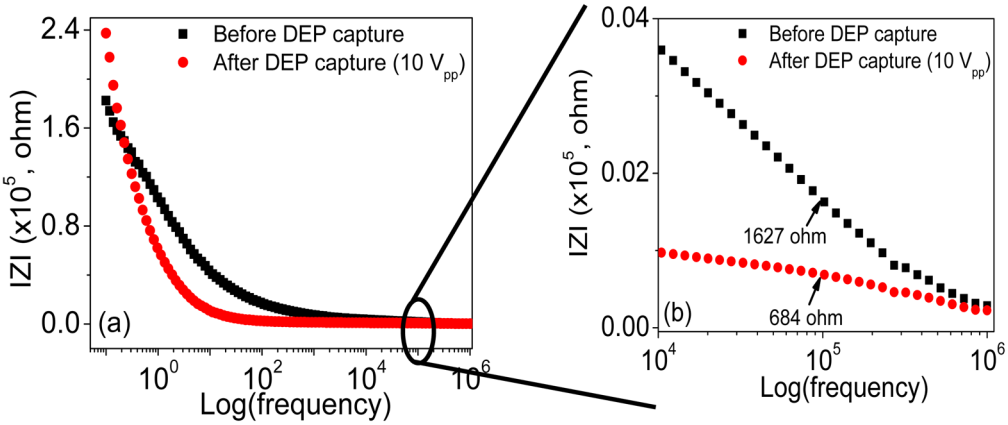

Figure 5.

Variation of the electrochemical impedance spectroscopy (EIS) before and after bacterial cell capture. (a) The Bode plot of the EIS, that is the amplitude of |Z| vs. the logarithm of the AC frequency, recorded in an *E. coli* cell suspension in deionized water before and after subjected to DEP capture at the exposed CNF tips by applying an AC potential of 10 V_{pp} at 100 kHz frequency. (b) An enlarged portion of the Bode plot to show impedance change at the frequency around 100 kHz in an *E. coli* cell suspension before and after subjected to DEP capture at the CNF NEA.